Effect of the Synthesis Initiation Mode on the Structure and Properties of Sulfadiazine Molecularly Imprinted Polymers

Zhiliang Zhang, Bing Wang, Jian Li

Key Laboratory of Hollow Fiber Membrane Materials and Membrane Processes (Ministry of Education), School of Environmental and Chemical Engineering, Tianjin Polytechnic University, Tianjin, China 300160

Received 9 February 2009; accepted 16 May 2010
DOI 10.1002/app.32834
Published online 24 September 2010 in Wiley Online Library (wileyonlinelibrary.com).

ABSTRACT: In the presence of imprinting molecules of sulfadiazine, two kinds of molecularly imprinted polymers (MIPs) were synthesized by photoinitiated and thermally initiated polymerizations, respectively. The combination of sulfadiazine and α-methyl acrylic acid and their composite ratio were studied by differential UV absorption spectrometry. The results show that a combined effect between the functional monomer and the imprinting molecule occurred in the solution. The structure and properties of these synthetic polymers were researched and compared with IR spectroscopy, transmission electron microscopy, and a balanced combination of static experiments. The polymer materials synthesized in these two ways had the same molecular structure, but their morphology was different. Furthermore, through the adsorption isotherm, Scatchard analysis, and evaluation of the imprinting efficiency, we determined that the lower temperature was a more suitable synthesis condition for the polymerization of the MIPs.
 J Appl Polym Sci 119: 3189–3198, 2011

Key words: functionalization of polymers; separation of polymers; separation techniques

INTRODUCTION

The molecular imprinting technique can be used to synthesize crosslinked polymers with memory effects for the three-dimensional structure of a specific molecule. It has been exploited extensively in many different applications, including separation materials, chemical sensors, reaction catalysts, and enzyme mimics.[1–9] In particular, the practical application of a matrix or medium material for drug separation and analysis has become a spectacular subject.[10–14]

It is known that the degree of specificity in molecularly imprinted polymers (MIPs) depends heavily on the polymerization process and on the nature of the ingredients, such as crosslinking agents, initiators, and solvents. So far, MIPs have been synthesized by thermal polymerization and photopolymerization. In these two methods, the temperature and pressure factors of the reaction system have a certain impact on the structure and properties of the polymers. In this study, sulfadiazine was selected as the imprinted molecule. In addition, α-methyl acrylic acid (MAA) was used as the functional monomer, and ethylene glycol dimethacrylate (EGDMA) was the crosslinker. Then, two different approaches, photoinitiation and thermal initiation, were used to synthesize the MIPs. The structure and properties of these synthetic polymer materials were compared through a variety of means that explained the influence of the synthesis conditions on the selective adsorption properties of the polymers; this study also provided new evidence for determining the molecular recognition mechanism of the molecular imprinting technique.

Drug separation and analysis is of great significance for clinical medicine, drug delivery *in vivo*, pharmacokinetics, the manufacturing and inspection of medicine, and so on. The exploitation of new selective materials for drug separation and analysis has a high value in applications. MIPs, with their excellent molecular recognition performance and stable physical and chemical properties, are considered good materials for drug analysis and separation. Sulfadiazine, the drug of first choice for curing epidemic encephalitis because it can be used for the treatment of pneumococcus, hemolytic streptococcus, and meningitis streptococcus infections, has a good imprintogenicity. So, in theory, it could be the template molecule for the preparation of a molecular imprinting material. In this experiment, α-methyl methacrylate and EGDMA, which are common and easy to get, were chosen for the functional monomer

Correspondence to: B. Wang (bingwang666@yahoo.com.cn).
Contract grant sponsor: Natural Science Foundation of Tianjin; contract grant number: 10JCZDJC21900.

and crosslinker, respectively, to prepare imprinted polymers. The synthetic material made a foundation for the qualitative and quantitative analysis of sulfadiazine. Then, we expected that a new effective separation and analysis method would be found for the purpose of controlling the drug dosage of sulfadiazine taken by patients or for detecting its content in human bodies to meet the best efficacy and minimal side effects, such as anaphylaxis, liver and renal toxicity, and fetal abnormity, in the future.

EXPERIMENTAL

Materials and reagents

Sulfadiazine (SD) was obtained from Beijing Bailingwei Chemical Technology Co., Ltd. (Beijing, China, 99%). MAA was supplied by Tianjin Chemical Reagent Research Institute (Tianjin, China). EGDMA was purchased from Shanghai Haiqu Chemical Co., Ltd. (Shanghai, China). All of the monomers were previously purified by vacuum distillation to remove inhibitors. 2,2′-Azobisisobutyronitrile was a product of Tianjin No.2 Chemical Reagent Factory (Tianjin, China) and was used as received. *N*,*N*-Dimethylformamide (DMF), methyl alcohol, acetic acid, anhydrous ethanol, and other chemicals were analytical grade and were obtained from commercial sources.

Main apparatuses

All UV–Visible spectra and adsorption experiments were performed with a UV-240 dual-wavelength UV–Visible spectrophotometer (Shimadzu, Tokyo, Japan). The IR spectrum analyses were done on a TENSOR37 Fourier transform infrared (FTIR) spectrometer (Bruker Corp., Karlsruhe, Germany). An H-7650 transmission electron microscope (Hitachi, Ltd., Tokyo, Japan) was used to observe the morphology of the imprinted polymers. To synthesize, prepare, and process the products, many other instruments were used, including a WE-1 thermostat water bath oscillator (Tianjin Honour Instruments, Inc., Tianjin, China), an SK5200 ultrasonic vibration generator (Shanghai Kudos Ultrasonic Instrument Co., Ltd., Shanghai, China), a TG16-WS (1650D) supercentrifuge (Shanghai Luxiangyi Centrifuged Instrument Co., Ltd., Shanghai, China), a long-wave (365-nm) ultraviolet lamp (Tianjin Zijin Special Photo Source Co., Ltd., Tianjin, China), and a Soxhlet extractor.

UV spectrometry of mixture solutions of SD and the functional monomers

A series of solutions were prepared with a fixed concentration of SD (0.05 mmol/L) and various amounts of MAA in DMF. The ratios of the molar concentrations of SD to MAA among this set of solutions were 1 : 0, 1 : 1, 1 : 2, 1 : 3, 1 : 4, 1 : 5, 1 : 6, and 1 : 8. The solutions were shaken for about 4–5 h to achieve sufficient interaction. The changes in the absorbance and difference absorption spectra of these solutions were determined on the UV spectrometer with a corresponding MAA–DMF solution as the reference. The results were used for further analysis.

Synthesis of the SD MIPs

SD (0.50056 g, 2 mmol) and the functional monomer (MAA, 0.51 mL, 6 mmol) were dissolved in 30 mL of DMF in a 50-mL glass ampule. After 6 h of oscillation, 5.64 mL (30 mmol) of crosslinker (EGDMA) and 40 mg of initiator (2,2′-azobisisobutyronitrile) were added. The solution was degassed in a sonicating bath and deoxygenated with a stream of nitrogen for 10 min. Then, the ampule was placed into an ice bath apparatus and sealed *in vacuo*. The polymerization was allowed to carry out in a constant water bath at 55°C or under a UV lamp (365 nm) at 5°C for 24 h. The resulting rigid polymers were ground to pass through a 74-μm sieve. Fine particles were removed by decantation in acetone. The resulting particles were placed in the Soxhlet extractor and washed with a 10% acetic acid–methanolic solution until the template could no longer be detected in the elution. Then, the particles were washed with pure methanol to remove residual acetic acid and dried to a constant weight *in vacuo* at 60°C. As a control, the nonimprinted polymer (NIP) in the absence of the template were prepared and treated by the same method.

IR spectrometry of the synthetic polymers

The polymers were ground into a fine powder (grain diameter $\approx$ 0.054 mm). After they were dried completely, test samples were made by the pressed disc method with KBr. Then, we scanned them within the wave-number range 400–4000 cm^{-1} to obtain their IR spectra, respectively, using the TENSOR37 FTIR spectrometer. Then, the polymers' molecular structure were analyzed comparatively. The tested samples were MIPs and NIPs before and after they were eluted and were labeled as follows: M_1 = molecularly imprinted polymer before elution, M_2 = molecularly imprinted polymer after elution, N_1 = nonimprinted polymer before elution, and N_2 = nonimprinted polymer after elution (see Fig. 1).

Transmission electron microscopy (TEM) characterization of the MIPs

We put MIPs with a certain degree of fineness into ethanol to prepare a suspension of an appropriate

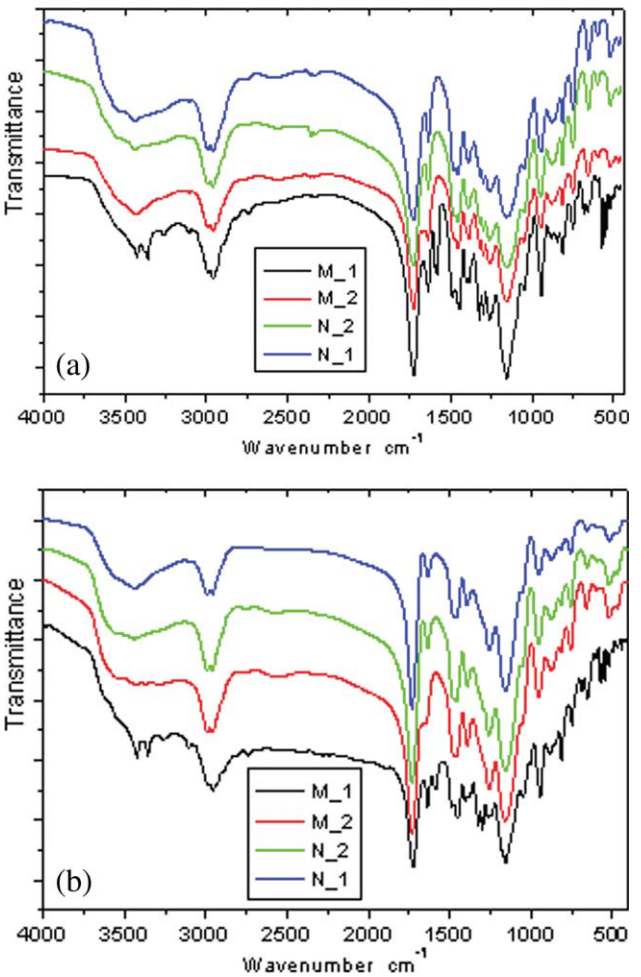

Figure 1 IR spectra of the polymer products synthesized by the (a) photoinitiation and (b) thermal initiation modes. [Color figure can be viewed in the online issue, which is available at wileyonlinelibrary.com.]

concentration (consistency = 5%) and scattered them for 15 min in the ultrasonic oscillator. Then, we used a professional copper net to quickly dredge the powder samples. After we removed the volatile ethanol absolutely, we observed the samples through TEM.

Isothermal adsorption experiment for the synthetic polymers

MIP (10 equiv) portions, for a mass of 100 mg, were put into a group of SD solutions with gradient concentrations of 0.25–7.00 mmol/L. After equilibrium was attained for all of the mixtures at 20°C, the mixtures were separated by centrifugation. Because the absorbency of the upper clear liquid could be determined with the quantitative measurement of UV absorption spectroscopy (λ = 273 nm), the mixture concentration could be fixed according to the standard curve. Then, the amount of SD bound to the imprinted polymer [Q(μmol/g)] was calculated by the following equation:

$$Q = (c_0 - c_t) \times V/m \quad (1)$$

where c_0 and c_t were the SD concentrations (mmol/L) measured at the initial time and the postinterval time (12 h) for equilibrium, respectively, and V and m are the volume of the SD solution (10 mL) and the weight of the dry polymer (100 mg) used for the adsorption experiment, respectively.

The adsorption volume of the NIP to SD could be measured in accordance with the same measured steps. According to the value of Q, the binding isotherm of the polymers and SD was drawn. The MIP and NIP, after the adsorption of sulfadiazine, was eluted in accordance with the method of molecular imprinting removal off the template and dried for reuse.

RESULTS AND DISCUSSION

Combination of MAA and SD as verified by UV spectroscopy

The affinity of MIPs to template molecules depends on the type of intermolecular forces, number of binding sites, and combining stability of functional monomers with template elements in the polymer solution. As reported in the literature on molecular imprinting, most interactions of combinations between the MIPs and substrates (also called *templates*) are in the form of electrovalent bonds or hydrogen bonds.[15] There are several amidocyanogens in SD molecules, which can form strong hydrogen bonds or ionic bonds with carboxylic acid in polar solvents. So MAA was chosen as the functional monomer to combine with the template molecules in this study. Their combination form was verified through differential UV absorption spectrometry in DMF solvent, and the appropriate amount of MAA was also determined at the same time.

In this experiment, the test solution samples were prepared at a fixed content of SD with gradual augmenting of the amount of MAA. These series of mixed solutions were scanned by a UV spectrometer with a corresponding concentration of MAA solution as the reference, respectively. The UV absorption spectra of SD with background correction for MAA and the solvent are shown in Figure 2.

As shown in Figure 3, with increasing amount of MAA, the maximum absorption peak intensity of SD decreased; moreover, its rate of decline decreased significantly. This was strong evidence for the supramolecular complex formed by MAA and SD. Because the group of MAA combined in the complex increased the steric hindrance of the benzene ring in the SD elements, the probability of electron transition decreased, and the absorbance was also reduced accordingly. According to the molecular

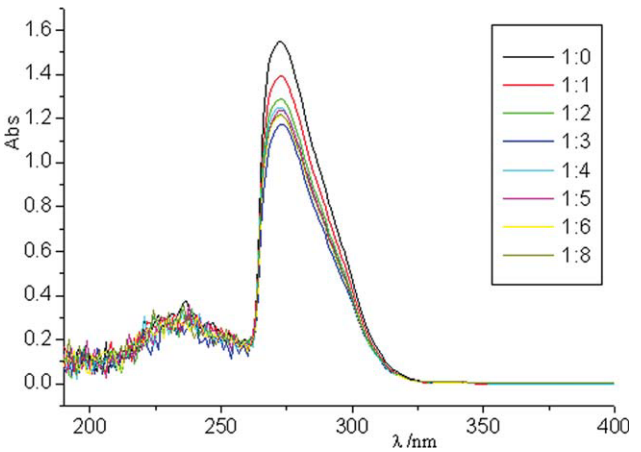

Figure 2 UV spectrograms of SD and SD–MAA with different SD–MAA molar ratios (which are listed in the figure). [Color figure can be viewed in the online issue, which is available at wileyonlinelibrary.com.]

structure of SD and MAA, we speculated further that H^+ of the carboxyl in the MAA element combined with N of the amido in the SD element to form NH^+, whereas the generated COO^- and NH^+ were driven together by electrostatic forces. In addition, N and O, which had lone-pair electrons, could have also engendered hydrogen bonds with O—H or N—H. These forces between molecules would have remodeled the electron density and distribution of the large π bond on the benzene ring in the SD molecule. As shown by results of the changes in the UV spectrum of SD, SD had strong interactions with MAA in DMF when the amount of MAA is appropriate. Therefore, it was possible to successfully prepare MIPs.

As shown by a comparison of the absorbance in maximum absorption wavelength, when MAA was at a certain concentration (three times that of SD), the absorbance dropped to the smallest value (shown in Fig. 3), that is, the absorption peak intensity of the minimum; when the concentration of MAA continued to increase, there was little pickup in the absorption, and ultimately, there was a balance in a larger concentration (over about six times that of SD), which showed the basic stability of the interaction between MAA and SD.

The greater the amount of MAA used was, the more obvious the changes were that were reflected in the UV absorption spectra of SD. They indicated that when the proportion of functional monomers was increased, their self-assembly with the template molecule were carried out more fully. However, it was not always better with a bigger proportion of functional monomer. In this experiment, when the ratio of MAA to SD was over 3 : 1, the absorption peak intensity went up and then declined slowly. After it was more than 6 : 1, the basic balance rose. This was because combination in competitive action and synergistic effects of the excessive functional monomers may have possibly occurred on the binding site (see Fig. 4). Thereby, we determined the ratio of imprinted molecule to functional monomer in the synthesis process to have a decisive impact on the products and their specific identifying properties. The appropriate amount of functional monomer can enhance the role of combination. However, excessive monomer can make matters worse. On the one hand, an excessive amount of functional monomer could lead to nonselective binding sites produced by the nonassembly of monomer functional residues. On the other hand, too much monomer can lead to its own association, which results in a decrease in selective binding sites instead. Thus, we used a molar ratio of n_{SD}–n_{MAA} of 1 : 3 in the synthesis of the sulfadiazine-imprinted polymer (n_{SD}, n_{MAA} were the molar quantity of SD and MAA, respectively).

Structural analysis of the polymers by IR spectroscopy

The information from the IR absorption spectra, such as the position, shape, and intensity of the absorption peaks, gave us access to the relevant structure of the molecules. In this experiment, IR analysis was applied to the characterization of the synthetic polymer structure and the certification of functional groups existing in the molecules. The IR spectra of the products are shown in Figure 1.

There are four spectral lines in these two figures, where lines marked as M_1 and N_1 correspond to the MIP and NIP before elution, respectively, and lines M_2 and N_2 correspond to the MIP and NIP after elution. These eight lines almost have similar absorption peak forms in each district, except for line M_1.

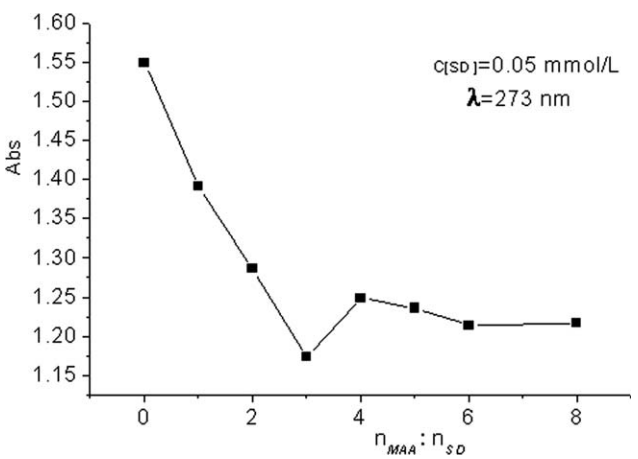

Figure 3 Absorbance changes of the maximum absorption peak for SD in mixed solutions with different molar ratios.

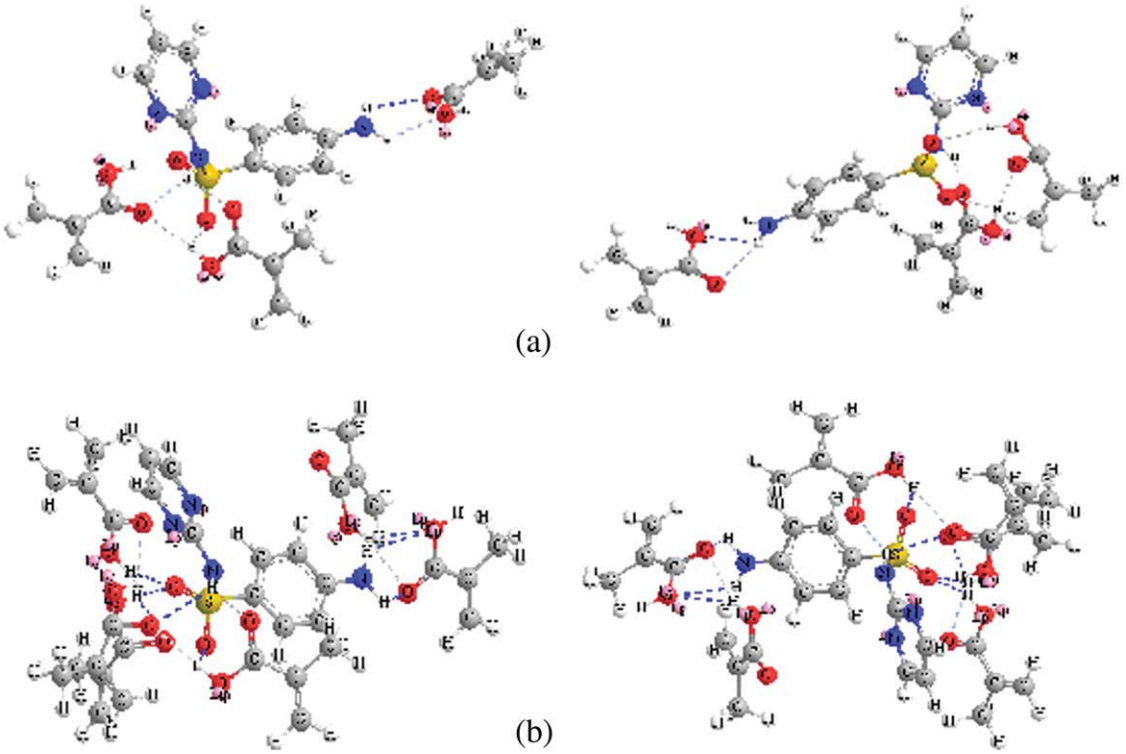

Figure 4 Supramolecular complex form of the template-functional monomer (SD–MAA) with nSD–nMAA ratios of (a) 1 : 3 and (b) 1 : 6. [Color figure can be viewed in the online issue, which is available at wileyonlinelibrary.com.]

We controlled the synthetic route of the polymers and the molecular structure of the raw materials (see Schemes 1 and 2), and further analysis of the product IR was carried out.

Among them, the absorption peaks at 2958 cm^{-1} of all of the polymers arose from the C—H stretching vibration (υ_{C-H}), and the band at 1730 cm^{-1} was for the carbonyl group absorption both in MAA and in EGDMA ($\upsilon_{C=O}$). The absorption band around 1158 cm^{-1} was attributed to the C—O ester group of EGDMA (υ_{C-O}), although the wide absorption band around 3435 cm^{-1} or so corresponded to the stretching vibration of O—H in carboxyl groups (υ_{O-H}). The existence of this molecular structure proved that the products of the crosslinked copolymer were synthesized by EGDMA and MAA under these experimental preparation conditions. The obtained polymers did have the functional group (carboxylic acid group) to match with the element sulfadiazine.

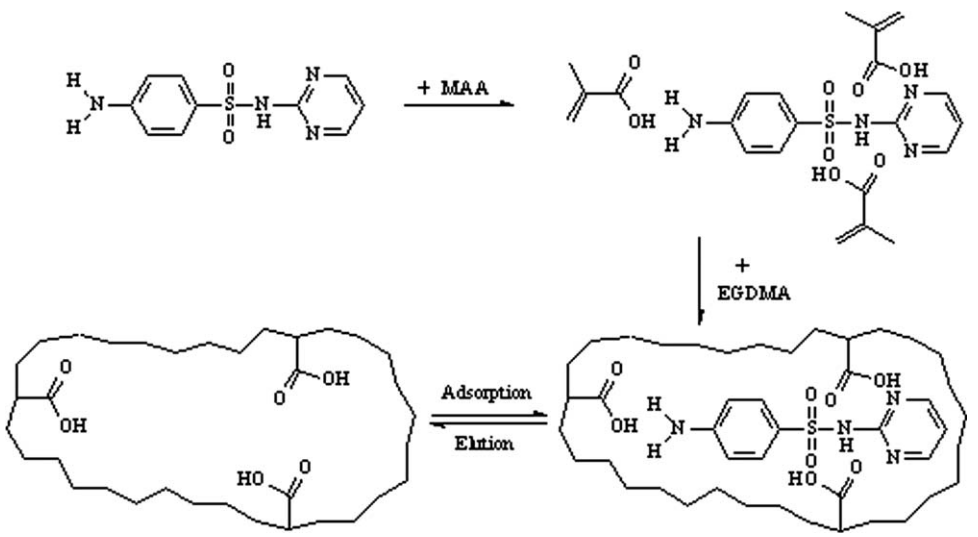

Scheme 1 Schematic representation for the synthesis of sulfadiazine-imprinted polymer.

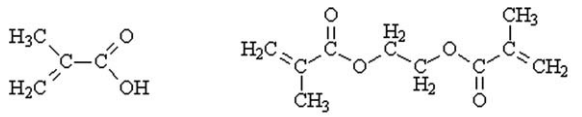

Scheme 2 Schematic representation for the molecular structures of MAA and EGDMA.

In addition, lines M_1 and M_2, showing the MIP before and after elution, were different. There were a few absorption peaks, with more appearing at 3357, 1595–1582, 881, 681, and 571–549 cm^{-1}. The original peaks in the 3435, 1390, and 1322-cm^{-1} regions, which seemed to be identical in all of the spectra, exhibited a subtle difference on a closer look. This was due to elements of sulfadiazine existing in the system. They were assigned to the stretching vibration of N—H (υ_{N-H}*3357*), skeleton vibrations of the benzene ring, and bending (rocking or twisting) deformation of C—H in the benzene ring ($\omega_{N-H} = 681\ cm^{-1}$, $\upsilon_{C-N} = 1390\ cm^{-1}$, and $\upsilon_{SO2} = 1322\ cm^{-1}$, respectively). This suggested that sulfadiazine molecules were successfully introduced into the MAA–EGDMA copolymer through imprinted molecule–functional monomer complexes. They could also be eluted off to make MIPs with the properties of identification and readsorption for the imprinting molecule. Polymers synthesized in the two initiated modes were nearly identical in the IR spectrum. That is, these two approaches resulted in products with the same molecular structure.

Morphology of the MIPs characterized by TEM

TEM successfully revealed the correlation between the macroproperties and microstructure of materials. Figure 5 shows the micromorphology of the MIPs observed with TEM.

As shown in Figure 5, the high-crosslinked polymers synthesized by the molecular imprinting technique were porous materials with a three-dimensional meshwork structure. There were nanomeshes in both MIPs. In some of the larger mesh, there were still holes in even smaller sizes. They spread good channels for solute diffusion and mass transfer. In addition, the MIP [Fig. 5(a)] had a more obvious pore structure than the NIP [Fig. 5(b)] synthesized in the photoinitiated polymerization, but the morphology of the MIP [Fig. 5(c)] and NIP [Fig. 5(d)] synthesized in the thermal initiation mode showed a similar structure.

When we compared Figures 5(a) and 5(c), we observed that the porous polymers prepared by photoinitiated and thermally initiated polymerization were with a certain level of pore size distribution. They not only had pores less than 10 nm but also some larger than 500 nm, and most of the pores were about 100–200 nm. These meshes provided a good space for the spread of solute and an important location for mass transfer. Meanwhile, the thermally initiated polymer, in contrast to the one synthesized in the photoinitiated polymerization, had a greater pore volume, surface area, and pore size, in which small pores less than 10 nm could hardly be found, relatively. This was due to a high temperature in the polymerization system, which could prepare polymers in large meshes and make a higher vapor pressure for the solvents and a stronger effect on the pore formation. In addition, the difference in the pore size between the molecularly imprinted polymer synthesized by the thermal initiation mode (MIP_Th) and the nonimprinted polymer synthesized by the thermal initiation mode (NIP_Th) was less obvious than that of the molecularly imprinted polymer synthesized by the photoinitiation mode (MIP_Ph) and the nonimprinted polymer synthesized by the photoinitiation mode (NIP_Ph). This may have also been because the solvent in the high-temperature polymerization systems had a strong porogen action, and the imprinted molecule had a relatively weaker effect on the polymer structure; this resulted in a poor imprinting effect of MIP_Th. To this end, there was reason to believe that changes in the structure of the polymers, along with the synthesis temperature, was also one of the important reasons for the ability to identify specifics of the MIP.

In short, there was a certain pore size distribution in the polymers synthesized by both the thermal and photoinitiation modes and a greater structure difference between MIP_Ph and NIP_Ph. Because the pore structure was an important factor in the performance of the MIPs, these polymers were continually taken as the research object in the following research. Through an experiment of balanced combination, their selective adsorption performance was studied and analyzed; this further illustrated that the pore structure factors played a very important role in the molecular imprinting separation.

Analyses of the adsorption properties and evaluation of the imprinting efficiency for the MIPs

In this experiment, the equilibrium adsorption capacity (Q) of the imprinted polymers to SD at different initial concentrations (range = 0.25–7.00 mmol/L) was determined with an equilibrium binding experiment method. The adsorption isotherm drawn from the experimental data is shown in Figure 6.

As shown in Figure 6, with increasing initial concentration, the adsorption capacity of both the MIP and NIP to the substrate increased. However, the

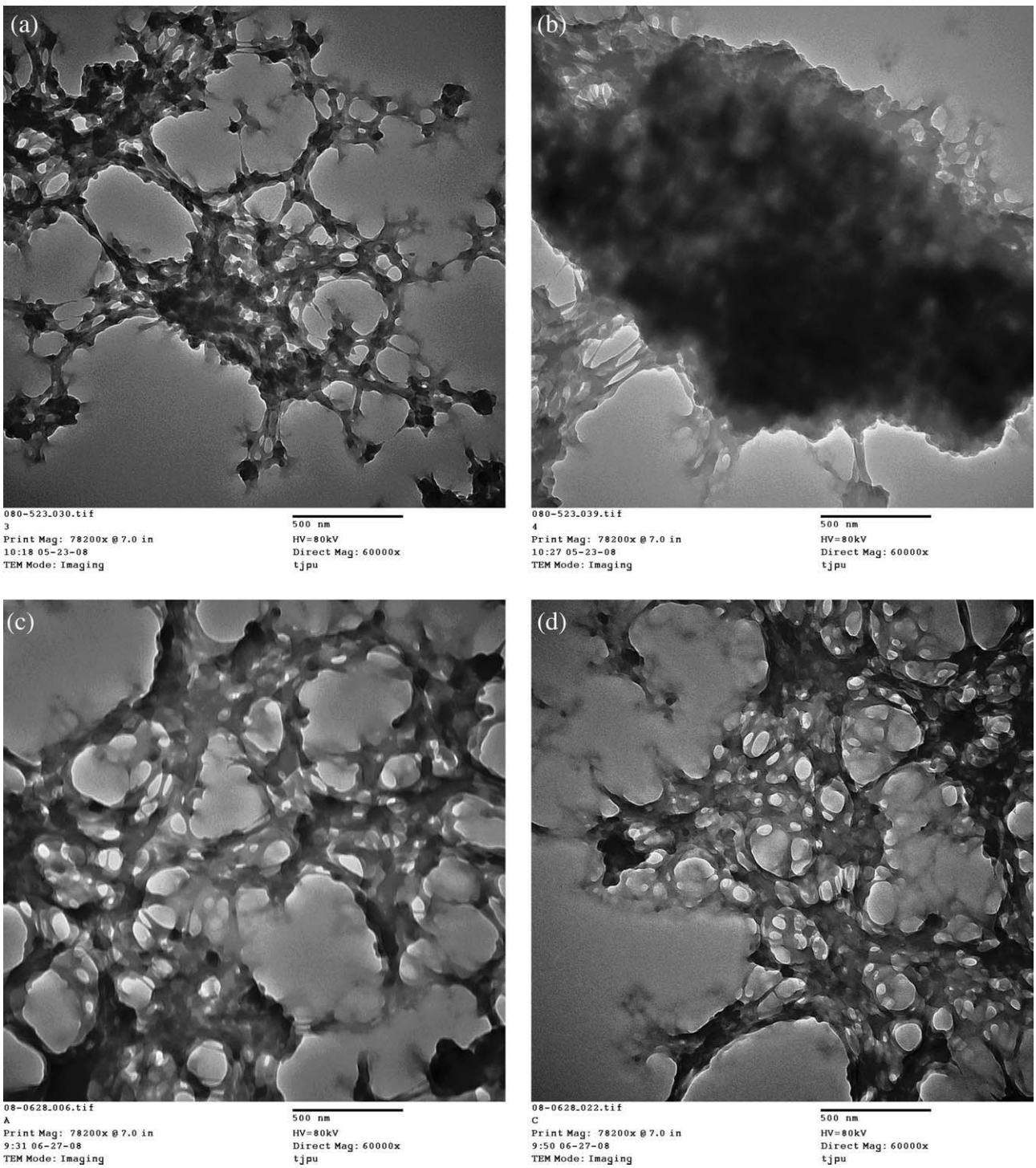

Figure 5 TEM images of the polymers (60,000×).

combination amount of the template molecules on the MIP was always greater than that of the NIP, obviously. Also, it would have been saturated in a high-concentration range. Thus, it showed a more advantageous binding ability. In many receptor binding assays,[16] because the curve of nonselective combined volume to the initial concentration increases linearly, it is difficult to reach saturation as a rule. This graph inferred that the adsorption of the NIP on SD was nonselective, and the MIP exhibited selective adsorption. This was because many specific structure holes with a fixed three-dimensional shape and position of functional groups matching SD formed during the synthesis process in the presence of the imprinted molecule. These imprinted holes with active binding sites caused a good ability for selective binding on the MIP. It also proved that the property of interaction force between the imprinted

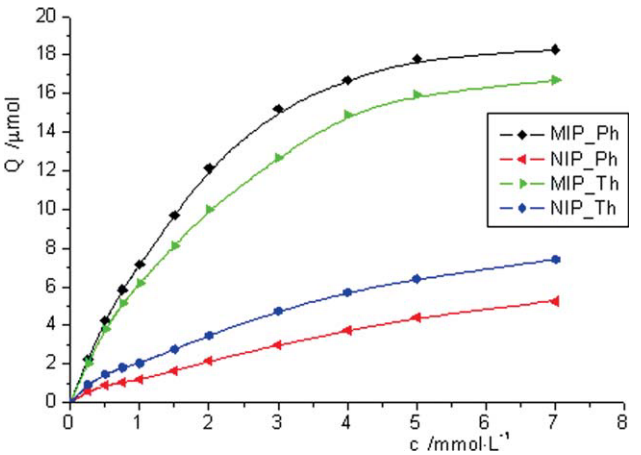

Figure 6 Adsorption isotherm of the imprinting molecule on the MIP and NIP. [Color figure can be viewed in the online issue, which is available at wileyonlinelibrary.com.]

molecule and functional monomer, when they presented as supramolecular complex in the course of synthesis, played an important role in the specific identification and strong affinity.

In the study of the molecular imprinting technique, the Scatchard model is often used to evaluate the MIP adsorption characteristics, and the Scatchard equation is as follows, according to the theory:[17,18]

$$Q/c\ [SD] = (Q_{max} - Q)/K_d \tag{2}$$

where K_d is defined as the equilibrium dissociation constant of the binding sites (mmol/L), Q is the amount of sulfadiazine bound to the polymer (μmol/g), Q_{max} is the apparent maximum number of binding sites, and c [SD] is the equilibrium concentration of sulfadiazine in the solution (mmol/L).

The experimental data were plotted in the coordinate graph of Q/c [SD] with Q. On the basis of the previous equation, straight lines were obtained for the linear fit, whose slope and intercept could be used to calculate the K_d and Q_{max} values of the binding site.

As shown in Figure 7, there were two distinct sections within the plot that could be regarded as straight lines. This suggested that there were two classes of heterogeneous binding sites with respect to the affinity for SD in this polymer. The linear equations and regression coefficients (correlation coefficients) are listed in Table I.

As judged by this phenomenon, within the studied extent of the SD concentration, the MIP mainly presented two different types of binding sites, which is a common result with MIPs. The cause of these two types of adsorption sites might have been that there may have been two inequable modalities of complex combined in a variety of interactions between the imprinting molecule and the functional monomers in the solution of the reaction mixture before and during the polymerization. Both of them were able to enter the cavity in the polymer matrix in different periods of the process. Then, they could have been crosslinked by the crosslinking agent and fixed in the copolymer. After the imprinting molecules were eluted, these two different adsorption properties of the binding sites formed in the MIP.

According to historical reports, Wang et al.[19] put forward the apparent imprinting efficiency (E_{ia}) and the practical efficient imprinting efficiency (E_i), which could be used as evaluations of the efficiency during the imprinting process and the proportion/percentage of the molecules successfully imprinted on the MIP, respectively. Their definition formulas are as follows:

$$E_i a = B_m/Q_i \tag{3}$$

$$E_i = (B_m - B_n)/Q_i \tag{4}$$

where Q_i is the theoretical maximum number of imprinted sites on the MIP and B_m and B_n are the apparent maximum numbers of binding sites on the MIP and NIP, respectively.

The imprinting efficiency of the MIPs synthesized in this study was evaluated after the adsorption performance test according to the aforementioned methods. The data of calculation and the results are listed in Table II

As shown in the previous data, MIP_Ph, which was synthesized with the same ratio of raw materials as MIP_Th, had a greater adsorption capacity, better selectivity, and more efficient imprinting efficiency. Thus, MIP prepared under conditions of low temperature showed a higher molecular recognition for the template. This indicated that the synthesis method of photoinitiated polymerization at low

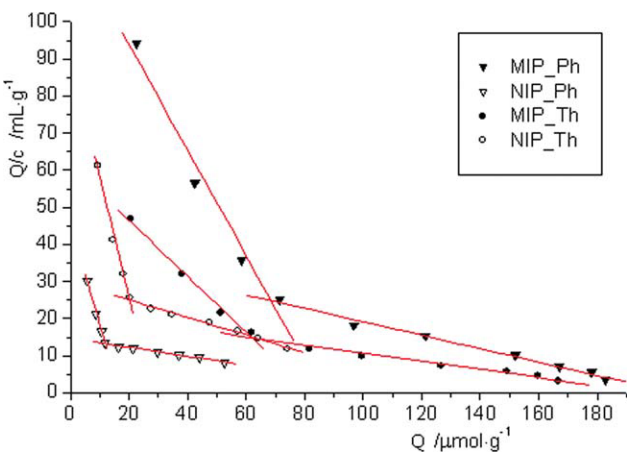

Figure 7 Scatchard plot analysis for the binding of SD to the imprinted polymer. The data is from the isothermal adsorption experiment. [Color figure can be viewed in the online issue, which is available at wileyonlinelibrary.com.]

TABLE I
Results of the Scatchard Analysis

Polymer	$Y = A + BX$	R	$K_d = -1/B$(mmol/L)	$Q_{max} = -A/B$(μmol/g)	$B = Q_{max1} + Q_{max2}$ (μmol/g)
MIP_Ph	$Y = 122.23275 - 1.41912X$	0.98626	0.70466	86.13278	292.21354
	$Y = 37.17903 - 0.18041X$	0.99424	5.54293	206.08076	
NIP_Ph	$Y = 45.84507 - 2.73292X$	0.99914	0.36591	16.77512	138.28433
	$Y = 14.71112 - 0.12107X$	0.99344	8.25968	121.50921	
MIP_Th	$Y = 61.50651 - 0.75217X$	0.99571	1.32949	81.77209	279.23676
	$Y = 21.79615 - 0.11038X$	0.98352	9.05961	197.46467	
NIP_Th	$Y = 90.9589 - 3.24772X$	0.99476	0.30791	28.00700	153.50038
	$Y = 29.86617 - 0.23799X$	0.99483	4.20186	125.49338	

temperatures might be more suitable for the imprinting process synthesis.

Before and during the process of polymerization, the functional monomer and imprinted molecule formed a supramolecular complex by the chemical interaction of noncovalent bonds. Those functional groups provided MIPs for binding sites with memory to the imprinted element. This was the reason for the selective adsorption of MIPs to the imprinted molecule. The stronger these noncovalent interactions were, the more stable the supramolecular complex was and the more it improved the specificity of the MIPs. The force of the chemical interaction between the functional monomer and the imprinted molecule was strengthened at lower temperatures. However, thermal polymerization was triggered at a high initial temperature. It weakened the interaction, which led to the reduction of memory of the site in the synthetic polymers. This was because the increase of molecular internal energy at high temperature in thermal polymerization process caused intense molecular motion, which thereby weakened the interaction between the template molecule and the functional monomers, so the memory site in the MIPs decreased. In the end, the product showed a little poorer identification adsorption properties than the one synthesized in the low-temperature environment.

In addition, the temperature also had a very complicated impact on the process of polymerization in the dynamics. The high-temperature led to a high synthesis rate, but it also led to a low degree of polymerization, which was due to the heat-generated nonuniformity. Moreover, the spatial arrangement of these polymeric chains was different from the corresponding products prepared at low temperature because the reorganization ability of the MIPs depended, to a large extent, on the part of the chain arranging into the space to fix and memorize the shape of the imprinting molecule. This might have been another reason the product of the photoinitiated polymerization at low temperature had a higher imprinting efficiency.

TABLE II
Evaluation of the Imprinting Efficiency

Polymer	Q_i (μmol/L)	B_m (μmol/g)	B_n (μmol/g)	E_{ia} (%)	E_i (%)
MIP_Ph	309.45	292.21	138.28	94.43	49.74
MIP_Th	309.45	279.24	153.50	90.24	40.63

CONCLUSIONS

In summary, with MAA as the function monomer and EGDMA as the crosslinker in the presence of SD as a molecular template, MIPs were prepared by two polymerization approaches: thermal initiation and photoinitiation.

The complex effect of the imprinting molecule and functional monomer was by UV spectroscopy before polymerization. The molecular structure of the synthetic product was analyzed by FTIR spectroscopy. This confirmed MIPs with molecular recognition and specific adsorption. Through TEM, the pore structure of the MIPs, which showed some difference between the MIP and NIP, was characterized. Among them, polymers synthesized by the photoinitiation approach were more different than the thermally initiated ones. The results of isothermal adsorption showed that the imprinted molecules could be absorbed in holes of the MIPs, and the products of the two methods showed a certain degree of difference in performance. Those findings not only explain the reasons the MIPs prepared by UV had more effective recognition ability but also prove that the spatial structure of the MIPs played a very important role during the process of molecular recognition.

References

1. Matsui, T.; Osawa, Y.; Shirasaka, K.; Katayama, M.; Hishiya, T.; Asanuma, H.; Komiyama, M. J Inclusion Phenom Macrocycl Chem 2006, 56, 39.
2. Lanza, F.; Sellergren, B. Chromatographia 2001, 53, 599.
3. Martín-Esteban, A. Fresenius J Anal Chem 2001, 370, 795.
4. Yoshikawa, M. Bioseparation 2002, 10, 277.
5. Silvestri, D.; Barbani, N.; Cristallini, C.; Giusti, P.; Ciardelli, G. J Membr Sci 2006, 282, 284.
6. Li, W.; Li, S. Adv Polym Sci 2007, 206, 191.

7. Dickert, F. L.; Forth, P.; Lieberzeit, P. A.; Voigt, G. Fresenius J Anal Chem 2000, 366, 802.
8. Becker, J. J.; Gagné, M. R. Acc Chem Res 2004, 37, 798.
9. Dickert, F. L.; Lieberzeit, P.; Tortschanoff, M. Sens Actuators B 2000, 65, 186.
10. Jin, H.; Wang, J.; Zhang, L.; Wu, X.; Zhang, W.; Chen, Z. Environ Prot Chem Ind 2006, 26, 295.
11. Zhang, L.-L.; Peng, T.; Wang, L.; Wang, Z.-P. Chem Eng 2004, 18, 48.
12. Kandimalla, V. B.; Ju, H. Anal Bioanal Chem 2004, 380, 587.
13. Verm, R. E.; Goody, R. J. Chromatographia 1999, 50, 407.
14. Sreenivasan, K. Bioseparation 2002, 10, 395.
15. Jiang, Z.; Wu, H. Molecular Imprinting Technique; Chemical Industry Press: Beijing, 2003; p 6.
16. Hawkins, D. M.; Trache, A.; Ellis, E. A.; Stevenson, D.; Holzenburg, A.; Meininger, G. A.; Reddy, S. M. Biomacromolecules 2006, 7, 2560.
17. Scatchard, G. Ann New York Acad Sci 1949, 51, 660.
18. Scatchard, G.; Scheineberg, I. H.; Armstrong, J. S. H. J Am Chem Soc 1950, 72, 535.
19. Wang, X.; Xu, Z.; Bing, N. Chem World 2007, 4, 243.